



**HAL**  
open science

## Mitochondrial involvement and erythronic acid as a novel biomarker in transaldolase deficiency

Udo F.H. Engelke, Fokje S.M. Zijlstra, Fanny Mochel, Vassili Valayannopoulos, Daniel Rabier, Leo A.J. Kluijtmans, András Perl, Nanda M. Verhoeven-Duif, Pascale de Lonlay, Mirjam M.C. Wamelink, et al.

### ► To cite this version:

Udo F.H. Engelke, Fokje S.M. Zijlstra, Fanny Mochel, Vassili Valayannopoulos, Daniel Rabier, et al.. Mitochondrial involvement and erythronic acid as a novel biomarker in transaldolase deficiency. *Biochimica et Biophysica Acta - Molecular Basis of Disease*, 2010, 1802 (11), pp.1028. 10.1016/j.bbadis.2010.06.007 . hal-00623290

**HAL Id: hal-00623290**

**<https://hal.science/hal-00623290>**

Submitted on 14 Sep 2011

**HAL** is a multi-disciplinary open access archive for the deposit and dissemination of scientific research documents, whether they are published or not. The documents may come from teaching and research institutions in France or abroad, or from public or private research centers.

L'archive ouverte pluridisciplinaire **HAL**, est destinée au dépôt et à la diffusion de documents scientifiques de niveau recherche, publiés ou non, émanant des établissements d'enseignement et de recherche français ou étrangers, des laboratoires publics ou privés.

## Accepted Manuscript

Mitochondrial involvement and erythronic acid as a novel biomarker in transaldolase deficiency

Udo F.H. Engelke, Fokje S.M. Zijlstra, Fanny Mochel, Vassili Valayannopoulos, Daniel Rabier, Leo A.J. Kluijtmans, András Perl, Nanda M. Verhoeven-Duif, Pascale de Lonlay, Mirjam M.C. Wamelink, Cornelis Jakobs, Éva Morava, Ron A. Wevers

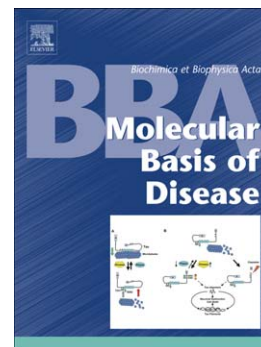
PII: S0925-4439(10)00117-1  
DOI: doi: [10.1016/j.bbadis.2010.06.007](https://doi.org/10.1016/j.bbadis.2010.06.007)  
Reference: BBADIS 63115

To appear in: *BBA - Molecular Basis of Disease*

Received date: 23 April 2010  
Revised date: 11 June 2010  
Accepted date: 11 June 2010

Please cite this article as: Udo F.H. Engelke, Fokje S.M. Zijlstra, Fanny Mochel, Vassili Valayannopoulos, Daniel Rabier, Leo A.J. Kluijtmans, András Perl, Nanda M. Verhoeven-Duif, Pascale de Lonlay, Mirjam M.C. Wamelink, Cornelis Jakobs, Éva Morava, Ron A. Wevers, Mitochondrial involvement and erythronic acid as a novel biomarker in transaldolase deficiency, *BBA - Molecular Basis of Disease* (2010), doi: [10.1016/j.bbadis.2010.06.007](https://doi.org/10.1016/j.bbadis.2010.06.007)

This is a PDF file of an unedited manuscript that has been accepted for publication. As a service to our customers we are providing this early version of the manuscript. The manuscript will undergo copyediting, typesetting, and review of the resulting proof before it is published in its final form. Please note that during the production process errors may be discovered which could affect the content, and all legal disclaimers that apply to the journal pertain.



## MITOCHONDRIAL INVOLVEMENT AND ERYTHRONIC ACID AS A NOVEL BIOMARKER IN TRANSALDOLASE DEFICIENCY

Udo F.H. Engelke<sup>1\*</sup>, Fokje S.M. Zijlstra<sup>1</sup>, Fanny Mochel<sup>2</sup>, Vassili Valayannopoulos<sup>3</sup>, Daniel Rabier<sup>3</sup>, Leo A.J. Kluijtmans<sup>1</sup>, András Perl<sup>4</sup>, Nanda M. Verhoeven-Duif<sup>5</sup>, Pascale de Lonlay<sup>6</sup>, Mirjam M.C. Wamelink<sup>7</sup>, Cornelis Jakobs<sup>7</sup>, Éva Morava<sup>1</sup>, Ron A. Wevers<sup>1</sup>

<sup>1</sup>Radboud University Nijmegen Medical Centre, Department of Laboratory Medicine, Laboratory of Genetic Endocrine and Metabolic Diseases, Nijmegen, The Netherlands, <sup>2</sup>Hôpital de La Salpêtrière, Department of Genetics and INSERM UMR S975, Paris, France, <sup>3</sup>Hôpital Necker-Enfants Malades, Department of Metabolic Disorders, Paris, France, <sup>4</sup>SUNY Upstate Medical University, Department of Medicine, NY, USA, <sup>5</sup>University Medical Center Utrecht, Department of Metabolic and Endocrine Diseases, Utrecht and Netherlands Metabolomic Centre, The Netherlands, <sup>6</sup>Hôpital Necker, Centre de Référence des Maladies Héréditaires du Métabolisme, Paris, France, <sup>7</sup>VU University Medical Center, Department of Clinical Chemistry, Metabolic Unit, Amsterdam, The Netherlands.

Running title: <sup>1</sup>H-NMR spectroscopy of urine: Transaldolase deficiency

Key words: NMR spectroscopy, citric acid cycle intermediates, pentose phosphate pathway, transaldolase deficiency, polyols, sedoheptulose, erythronic acid, 2-oxoglutaric acid

\* Corresponding author:

E-mail: u.engelke@labgk.umcn.nl; fax +31-24-3668754

Radboud University Nijmegen Medical Centre, Department of Laboratory Medicine, Laboratory of Genetic Endocrine and Metabolic Diseases, Geert Grooteplein 10, 6525 GA Nijmegen, The Netherlands.

**Nonstandard abbreviations**

CSF	Cerebrospinal fluid
GC-MS	Gas Chromatography-Mass Spectroscopy
IEM	Inborn Error of Metabolism
LC-MS	Liquid Chromatography-Mass Spectroscopy
OMIM	Online Mendelian Inheritance in Man
PPP	Pentose Phosphate Pathway
RPI	Ribose 5-Phosphate Isomerase
TALDO	Transaldolase
TLC	Thin Layer Chromatography
TSP	Trimethylsilyl-2,2,3,3-tetradeuterium propionic acid

**ABSTRACT**

*Background:* Sedoheptulose, arabitol, ribitol and erythritol have been identified as key diagnostic metabolites in TALDO deficiency.

*Method:* Urine from 6 TALDO deficient patients and TALDO deficient knock-out mice were analyzed using  $^1\text{H-NMR}$  spectroscopy and GC-mass-spectrometry.

*Results:* Our data confirm the known metabolic characteristics in TALDO deficient patients. The  $\beta$ -furanose form was the major sedoheptulose anomer in TALDO deficient patients. Erythronic acid was identified as a major abnormal metabolite in all patients and in knock-out TALDO mice implicating an as yet unknown biochemical pathway in this disease. A putative sequence of enzymatic reactions leading to the formation of erythronic acid is presented. The urinary concentration of the citric acid cycle intermediates 2-oxoglutaric acid and fumaric acid was increased in the majority of TALDO deficient patients but not in the knock-out mice.

*Conclusion:* Erythronic acid is a novel and major hallmark in TALDO deficiency. The pathway leading to its production may play a role in healthy humans as well. In TALDO deficient patients there is an increased flux through this pathway. The finding of increased citric acid cycle intermediates hints towards a disturbed mitochondrial metabolism in TALDO deficiency.

**INTRODUCTION** Two new defects in the pentose phosphate pathway (PPP) have recently been discovered: ribose 5-phosphate isomerase (RPI) deficiency (OMIM 608611) and transaldolase (TALDO) deficiency (OMIM 606003).

The first and as yet only case of RPI deficiency was described by Huck et al. [1]. The patient was a 14-year-old boy with leukoencephalopathy and peripheral neuropathy. Magnetic resonance spectroscopy (MRS) showed elevated levels of the polyols ribitol and arabitol in the brain. Ten patients from six families with TALDO deficiency are known [2-5]. The disease is associated with liver symptoms, while other organs are affected to a variable degree [4;5]. The metabolic phenotype of this disease is characterized by increased urinary concentrations of the polyols erythritol, arabitol, ribitol, sedoheptitol, perseitol, the sugars sedoheptulose and mannoheptulose, and sedoheptulose-7-phosphate [4;6]. Erythritol, arabitol and sedoheptulose have been described as most prominent diagnostic metabolites in urine of patients.

The biochemical diagnosis of RPI and TALDO deficiency relies on finding strongly increased concentrations of polyols in body fluids. The use of LC-MS/MS, LC-MS, and GC-MS for this purpose has been reported [7-9]. <sup>1</sup>H-NMR spectroscopy can be used for identification and quantification of proton-containing metabolites in body fluids [10]. RPI deficiency was diagnosed successfully by measuring high concentrations of ribitol and arabitol in urine and cerebrospinal fluid (CSF) using NMR spectroscopy [11].

In this study, we had the opportunity to characterize urine from 6 patients with genetically confirmed TALDO deficiency. We show for the first time the presence of increased urinary erythronic acid in all TALDO deficient patients and show that this metabolite is a biochemical hallmark of TALDO deficiency. Furthermore resonances of the  $\beta$ -furanose anomer of sedoheptulose were identified and quantified in all urine NMR spectra of the TALDO patients.

## MATERIALS AND METHODS

**Patients:** 6 Patients from 4 families with TALDO deficiency were included in this study (Table 1). Clinical details about the patients 1-3 have been described elsewhere (patient 1 [2], patient 2 and 3 [12]). In patients 4, 5 and 6, the diagnosis TALDO deficiency was confirmed at the metabolite level and the molecular genetic level.

**Mice:** Urine from TALDO-deficient “knock-out” mice was obtained from Dr András Perl [7].

**Authentic standards:** Sedoheptulose is not commercially available and was isolated from the hybride plant *Sedum spectabile* “Brillant” [13]. Leaves and stalk (70 g wet weight) were homogenized in 100 mL water and centrifugated through a 10-kD filter to remove proteins. Subsequently, the ultrafiltrate was concentrated by evaporation. The resulting preparation was further isolated preparatively by thin-layer chromatography (TLC) essentially as described by Engelke et al. [10] and measured as a model compound by  $^1\text{H}$ -NMR spectroscopy and GC-MS and (Figure 1A and B, respectively).

Calcium L-threonic acid, potassium D-erythronic acid and sedoheptulose-7-phosphate are commercially available from TCI Chemicals (Portland, USA), Carbosynth (Berkshire, UK) and Sigma-Aldrich (St Louis, MO USA), respectively.

**Sample preparation:** The urine samples were centrifuged before analysis. A volume of 70  $\mu\text{L}$  of a 20.2 mmol/L trimethylsilyl-2,2,3,3-tetradeuteriumpropionic acid (TSP, sodium salt; Aldrich)  $^2\text{H}_2\text{O}$  solution was added to 700  $\mu\text{L}$  of urine as a chemical shift reference ( $\delta = 0.00$ ) and as a lock signal. The pH of the urine was adjusted to  $2.50 \pm 0.05$  with HCl. Finally, we placed 650  $\mu\text{L}$  of the sample into a 5 mm NMR tube (Wilmad Royal Imperial; Wilmad LabGlass, USA).

### One-dimensional $^1\text{H}$ -NMR spectroscopy and $^1\text{H}$ - $^1\text{H}$ COSY spectroscopy

The urine samples were measured at 500 MHz on a Bruker DRX 500 spectrometer essentially as described before [14]. The samples were spun (14 Hz) during the 1D measurement. Shimming of the

field homogeneity was satisfactory when the TSP line width at half peak height was smaller than 1 Hz. Phasing of the spectra was completed manually, and the baseline was corrected using a cubic spline function. Metabolite resonances were fitted semi-automatically with a Lorentzian line shape and the resulting areas were compared with area of creatinine singlet (3.13 ppm; the N-CH<sub>3</sub> protons) to determine metabolite concentrations expressed as  $\mu\text{mol}/\text{mmol}$  creatinine.

**GC-Mass spectroscopy** Monosaccharides and polyols were analyzed as trimethylsilyl derivatives by GC-MS essentially as described by Janssen et al. [9]. A VF-01 ms WCOT column (20m $\times$ 0.15mm $\times$ 0.15 $\mu\text{m}$ ) from Varian was used. The method is not optimally suited for quantification of sugar acids.

## Results

**Sedoheptulose.** The  $^1\text{H-NMR}$  spectrum of the isolated sedoheptulose in aqueous solution at pH 2.50 shows a complex pattern of resonances deriving from a mixture of furanose and pyranose anomers (Figure 1A). Resonance assignments were based on previously reported NMR spectra of sedoheptulose (The Human Metabolome Database (HMDB, <http://www.hmdb.ca>), HMDB ID 03219), sedoheptulose-7-phosphate [15], and simulated NMR spectra of four sedoheptulose anomers:  $\alpha$ -furanose,  $\beta$ -furanose,  $\alpha$ -pyranose and  $\beta$ -pyranose (ACD/HNMR Predictor, Advanced Chemistry Development, Inc., Toronto, Ontario, Canada). The  $^1\text{H-NMR}$  spectrum shows that the  $\beta$ -furanose form of sedoheptulose had the highest concentration of the four anomeric forms. This is in line with observations on the anomeric forms of sedoheptulose-7-phosphate ( $\alpha$ -furanose:  $\beta$ -furanose:  $\alpha$ -pyranose = 20%:60%:20%) [15;16]. As indicated in figure 1A (★), the NMR spectrum showed smaller resonances at 4.17, 4.00, 3.94, 3.65 and 3.48 ppm representing the other anomeric forms of sedoheptulose.  $^1\text{H-NMR}$  assignments for the  $\beta$ -furanose anomer of sedoheptulose are described in Table 2. The splitting pattern and order of shift are comparable with sedoheptulose-7-phosphate. GC-MS Analysis showed the presence of four sedoheptulose anomers with the furanose anomer as the most prominent form (Figure 1B). The furanose and pyranose anomers were identified by their characteristic  $m/z$  fragments (Figure 1C<sub>1</sub> and C<sub>2</sub>, respectively).

**Sedoheptulose in urine.** In Figure 2D, the urine  $^1\text{H-NMR}$  spectrum (4.4 – 3.4 ppm) from a 1-month-old TALDO patient is shown (Table 1, patient 2). Major metabolites in this region are creatinine (singlet at 4.29 ppm) and betaine (singlet at 3.97 ppm). Several unusual resonances were observed in this region (Figure 2D, resonances S<sub>1</sub>, S<sub>3</sub>, S<sub>4</sub>, E<sub>2</sub>, E<sub>3</sub> and E<sub>4</sub>). This pattern of resonances was found in the urine from all patients with TALDO deficiency and was not observed in NMR spectra of urine from 100 healthy children (age: 4 to 12 years). In TALDO deficiency, high  $\mu\text{molar}$  concentrations of sedoheptulose, erythritol and arabitol are present in the urine [4]. Comparison of the urine from patient 2 with the spectrum of the isolated sedoheptulose shows that the unusual resonances S were

caused by the  $\beta$ -furanose anomer of sedoheptulose (Figure 2C and D). Confirmation was provided by a 2D COSY NMR experiment on the isolated sedoheptulose and the urine sample of TALDO patient nr 2. Two characteristic cross peaks of sedoheptulose with the coordinates 4.08/4.29 and 4.29/3.75 ppm were observed in the 2 dimensional NMR urine COSY spectra of the TALDO patients. Quantification of  $\beta$ -furanose sedoheptulose was performed on the doublet at 4.08 ppm (Figure 2D, resonance S<sub>3</sub>) and was 1700  $\mu\text{mol}/\text{mmol}$  creatinine in patient 2. In TALDO-deficient patients the urinary concentration of  $\beta$ -furanose sedoheptulose ranged between 160 and 1700  $\mu\text{mol}/\text{mmol}$  creatinine (Table 1). The other three anomers of sedoheptulose ( $\alpha$ -furanose,  $\alpha$ -pyranose and  $\beta$ -pyranose) were not observed in a urine NMR spectrum of the TALDO patients due to their low concentration and overlap by other resonances in the region between 4.3 and 3.5 ppm. The resonances of sedoheptulose-7P could not be observed in a 1D proton NMR spectrum of urine of our patients due to the known low concentration of sedoheptulose-7P in TALDO patients (2 – 24  $\mu\text{mol}/\text{mmol}$  creatinine) and overlap by other resonances [6].

GC-MS analysis confirmed the presence of abnormally high concentrations of sedoheptulose in the urine of all TALDO patients. The relative abundance of its four anomeric form was similar for all TALDO urine samples and the sedoheptulose from sedum spectabile (Figure 1B). The mass spectrum shows a characteristic ratio for m/z 204 and 217 in the furanose and the pyranose anomers (Figure 1C; [17;18]). The m/z 217 is caused by a strong ion  $\text{RO-CH=CH-CH-O}^+\text{R}$  from furanoid hemiacetals while the m/z 204 derives from the  $(\text{RO-CH-})_2^+$  ion from pyranoid hemiacetals [18]. Comparison between the NMR data and the GC-MS profile makes it likely that the alfa-forms of furanose and pyranose anomers have a shorter retention time on this column than the beta-forms. In the GC-MS profile the anomeric ratios of sedoheptulose were found to be furanose : pyranose = 86% : 14% for urine of TALDO patients and 92% : 8% for the sedoheptulose isolated from sedum spectabile.

**Erythritol, ribitol and arabitol.** GC-MS Analysis of urine from TALDO patients shows elevated concentrations of erythritol, ribitol and arabitol (Table 1). The resonances of these polyols could not

be observed in either the 1D urine spectra or the 2D COSY NMR spectra. An explanation for this is that the protons of erythritol, ribitol and arabitol have a high degree of splitting [11]. Identification and quantification of these polyols is further hampered by overlapping resonances from other urinary metabolites in the region 4.0 - 3.5 ppm [11].

**Erythronic acid.** The other unknown resonances in the 1D spectrum (Figure 2D, resonances E<sub>2</sub>, E<sub>4</sub> and E<sub>3</sub>) could not be explained by the metabolites erythritol or arabitol. In order to identify resonances E, several NMR en GC-MS experiments were performed. COSY spectra revealed that the doublet resonance at 4.32 ppm was coupled with a resonance at 3.99 ppm. A NMR database (BRUKER, AMIX), containing spectra of 500 metabolites at various pH, revealed threonic acid as a candidate metabolite for the doublet resonance at 4.32 ppm. GC-MS analysis confirmed the presence of a high peak (with the same molecular weight of threonic acid (MW = 136)) in urine samples of the TALDO patients. However, spiking threonic acid to the urine and 1D NMR experiments at various pH values proved that the resonances at 4.32 and 3.99 ppm were not caused by threonic acid.

Erythronic acid is the diastereomer of threonic acid. The compound is commercially available and was purchased at Carbosynth (Berkshire, UK). Erythronic acid in H<sub>2</sub>O at pH 2.5 (Fig. 2B) showed resonances at 4.32 (doublet,  $J = 4.5\text{Hz}$ ), 3.69 (multiplet) and 3.99 (multiplet) ppm (Table 2). Quantification of erythronic acid in urine samples was performed on the single proton attached to the C2 (Figure 2D, resonances E<sub>2</sub>) and the TSP singlet at 0.00 ppm was used as the concentration reference. After spiking erythronic acid to a urine sample at a level of 5.8 and 10.7 mmol/l, the recovery amounted to  $\pm 90\%$ .

Erythronic acid in H<sub>2</sub>O at pH 2.5 (Fig. 2B) showed the same 1D and 2D resonance pattern as observed in the urine of the TALDO deficient patients. The addition of pure erythronic acid to the urine sample of TALDO patient 5 resulted in an increase of the doublet at 4.32 ppm. Additionally, 1D <sup>1</sup>H-NMR spectra of erythronic acid and the urine sample were recorded at pH 7.0. Both spectra showed a doublet resonance which shifted from 4.32 ppm (pH 2.50) to 4.10 ppm (pH 7.0). These

experiments confirmed the occurrence of erythronic acid in urine of TALDO deficient patients. The erythronic acid concentration ranged between 350 and 2900  $\mu\text{mol}/\text{mmol}$  creatinine in the TALDO-deficient patients. In a control group of 100 healthy children (age: 4 to 12 years), we never found erythronic acid levels higher than 50  $\mu\text{mol}/\text{mmol}$  creatinine, in line with results reported by General et al. [19]. In the urine from three newborns (age: 3 to 5 days), higher values up to 150  $\mu\text{mol}/\text{mmol}$  creatinine were found. Thus, erythronic acid occurs as a regular metabolite at low micromolar concentration in urine samples.

GC-MS analysis confirmed the presence of abnormally high concentrations of erythronic acid in the urine of TALDO patients. Figure 3 shows the GC-MS chromatogram of a control urine (Fig. 3C) and urine from TALDO patient (Fig. 3B). The retention time and the mass spectrum of the erythronic acid peak in the urine of the TALDO patients correspond with the model compound spiked to a pooled urine sample (Figure 3A).

**Other metabolic abnormalities.** In five out of six TALDO deficient patients the urinary concentration of 2-oxoglutaric acid was increased, varying between 50 and 1090  $\mu\text{mol}/\text{mmol}$  creatinine (reference ranges in  $\mu\text{mol}/\text{mmol}$  creatinine:  $\leq 5$  years=30-117,  $>5$  years = 2-95, adults=4-74 [20]). 2-Oxoglutaric acid was not increased in urine samples from TALDO patient 2. Fumaric acid was increased in four of the six TALDO-patients (patients 1, 2 3 and 6; Table 1). The urine of patient 6 (4-years-old) showed the highest concentration of 2-oxoglutaric acid (1090  $\mu\text{mol}/\text{mmol}$  creatinine) and fumaric acid (110  $\mu\text{mol}/\text{mmol}$  creatinine). The concentrations of other metabolites from the citric acid cycle, succinic acid and citric acid, were normal in all urine samples from the TALDO patients. Also lactate was normal in all TALDO urine samples and increased blood lactate has not been observed in these patients.

**TALDO deficient “knock-out” mice.** The urine from two TALDO-deficient “knock-out” mice were measured by 1D and 2D  $^1\text{H}$ -NMR spectroscopy and compared with the urine spectra from wild-type mice (Figure 4). The 1D spectra of the two TALDO deficient mice showed the presence of high concentrations of erythronic acid (1100 and 1700  $\mu\text{mol}/\text{mmol}$  creatinine) and of the  $\beta$ -furanose

anomer of sedoheptulose (2300 and 3000  $\mu\text{mol}/\text{mmol}$  creatinine). These findings are consistent with the results observed in the urine NMR spectra of the TALDO deficient patients. The  $\beta$ -anomer of sedoheptulose and erythronic acid were not observed in the urine NMR spectra of the wild-type mice. 2-Oxoglutaric acid and fumaric acid had a normal concentration in the urine of TALDO deficient and wild-type mice.

## DISCUSSION

$^1\text{H}$ -NMR spectroscopy provides an overall view of proton-containing metabolites present in body fluids. Therefore, *in vitro* NMR spectroscopy is suited to diagnose patients with inborn errors of metabolism [10;21]. This study describes the *in vitro* NMR investigations at the metabolite level on 6 patients with TALDO deficiency. The 1D and 2D COSY  $^1\text{H}$ -NMR spectra from these patients show a characteristic metabolic profile, mainly due to the resonances deriving from erythronic acid and the  $\beta$ -furanose anomer of sedoheptulose. GC-MS analysis confirmed the increased erythritol, ribitol and arabitol concentrations in the urine from the TALDO deficient patients. An increased concentration of erythronic acid in the urine of TALDO patients has not been described before. A low concentration of erythronic acid is always observed in urine from healthy children [19]. Our data show that on a molar basis, the excretion of erythronic acid is comparable to the sedoheptulose excretion. In this study, in 5 out of 6 TALDO deficient patients, the concentration of erythronic acid in urine was higher than the concentration of the metabolites sedoheptulose, erythritol, ribitol and arabitol. Therefore, erythronic acid ranks among the key metabolic features in TALDO deficiency and testifies a high flux through an as yet unknown metabolic pathway. As erythronic acid is always found in low concentration in the urine [19], the putative pathway shown in figure 5 may be present in healthy volunteers as well. The accumulation of erythronic acid in TALDO deficient patients can putatively be explained as shown in Figure 5. In TALDO deficiency the flux through the PPP is disturbed leading to the accumulation of sedoheptulose-7-phosphate [4]. Wamelink et al. [4] speculated that the accumulation of sedoheptulose-7-phosphate is further metabolized into sedoheptulose as a detoxification process. Sedoheptulose can further be metabolized to erythrose via the enzymes fructokinase and aldolase (Figure 5, enzyme 4 and 5 [22]). Subsequently, erythrose can be reduced to erythritol which is found in high concentration in the urine of TALDO deficient patients. Alternatively, erythrose may be phosphorylated into erythrose-4-phosphate as shown in Figure 5 step 7 [23]. Erythrose-4-phosphate can be a substrate for transaldolase in some cell types. Also erythrose-4-phosphate is a known substrate for glyceraldehyde 3-phosphate dehydrogenase, converting it to 1,4-bis-phosphor-

erythronate or to 4-phosphoerythronate [24;25]. In patients with TALDO deficiency the flux through this enzymatic reaction will increase. The next step in the formation of erythronic acid is most probably a dephosphorylation by one of the 'non-specific' phosphatases that are present in all cells. Erythrose may also be converted to erythronic acid via lactone formation (Figure 5, step 10) in a similar way as D-galactose can be converted in galactosaemia patients via d-galactono-lactone to D-galactonic acid. Confirmation of the pathway leading to erythronic acid by further experiments is required [26]. The availability of TALDO knock-out mice is an advantage in this respect.

In almost all TALDO deficient patients urinary fumaric acid and 2-oxoglutaric acid were elevated while lactate and other metabolites from the citric acid cycle such as succinic acid, malic acid were normal. The mechanism behind this accumulation of specific citric acid cycle intermediates remains to be elucidated. Via D-glyceraldehyde 3-phosphate, an intermediate of the glycolysis, an increased flux through the glycolysis towards the citric acid cycle may occur in TALDO deficient patients. However this would only lead to accumulating citric acid cycle intermediates when there is uncoupling of the citric acid cycle and the respiratory chain or when there is direct inhibition of specific citric acid cycle enzymes. The observation of increased citric acid cycle intermediates is of potential clinical interest. As yet hyperlactacidemia has not been observed in TALDO deficiency and to our knowledge extensive testing of the respiratory chain in muscle or liver of the patients has not been performed. Hanczko et al, however, did find evidence for mitochondrial dysfunction and oxidative stress in the liver of TALDO knock-out mice characterized by low NADPH, low glutathione, a low ATP/ADP ratio and accumulation of lipid hydroperoxides [27]. Our observations may be a starting point for further studies on mitochondrial aspects in human TALDO deficiency.

In conclusion, we have shown that NMR spectroscopy of urine can be used to diagnose patients with TALDO deficiency. The high urinary concentration of erythronic acid in TALDO patients has not been reported before and may serve as a new diagnostic hallmark of TALDO deficiency.

## Reference List

1. Huck JH, Verhoeven NM, Struys EA, Salomons GS, Jakobs C, van der Knaap MS. Ribose-5-phosphate isomerase deficiency: new inborn error in the pentose phosphate pathway associated with a slowly progressive leukoencephalopathy. *Am J Hum Genet* 2004;74:745-51.
2. Verhoeven NM, Huck JH, Roos B, Struys EA, Salomons GS, Douwes AC, van der Knaap MS, Jakobs C. Transaldolase deficiency: liver cirrhosis associated with a new inborn error in the pentose phosphate pathway. *Am J Hum Genet* 2001;68:1086-92.
3. Verhoeven NM, Wallot M, Huck JH, Dirsch O, Ballauf A, Neudorf U, Salomons GS, van der Knaap MS, Voit T, Jakobs C. A newborn with severe liver failure, cardiomyopathy and transaldolase deficiency. *J Inherit Metab Dis* 2005;28:169-79.
4. Wamelink MM, Struys EA, Jakobs C. The biochemistry, metabolism and inherited defects of the pentose phosphate pathway: a review. *J Inherit Metab Dis* 2008;31:703-17.
5. Tylki-Szymanska A, Stradomska TJ, Wamelink MM, Salomons GS, Taybert J, Pawlowska J, Jakobs C. Transaldolase deficiency in two new patients with a relative mild phenotype. *Mol Genet Metab* 2009;97:15-7.
6. Wamelink MM, Smith DE, Jansen EE, Verhoeven NM, Struys EA, Jakobs C. Detection of transaldolase deficiency by quantification of novel seven-carbon chain carbohydrate biomarkers in urine. *J Inherit Metab Dis* 2007;30:735-42.
7. Vas G, Conkrite K, Amidon W, Qian Y, Banki K, Perl A. Study of transaldolase deficiency in urine samples by capillary LC-MS/MS. *J Mass Spectrom* 2006;41:463-9.
8. Wamelink MM, Smith DE, Jakobs C, Verhoeven NM. Analysis of polyols in urine by liquid chromatography-tandem mass spectrometry: a useful tool for recognition of inborn errors affecting polyol metabolism. *J Inherit Metab Dis* 2005;28:951-63.
9. Jansen G, Muskiet FA, Schierbeek H, Berger R, van der Slik W. Capillary gas chromatographic profiling of urinary, plasma and erythrocyte sugars and polyols as their trimethylsilyl derivatives, preceded by a simple and rapid prepurification method. *Clin Chim Acta* 1986;157:277-93.
10. Engelke UF, Moolenaar SH, Hoenderop SMGC, Morava E, van der Graaf M, Heerschap A, Wevers RA. Handbook of  $^1\text{H}$ -NMR spectroscopy in inborn errors of metabolism: body fluid NMR spectroscopy and in vivo MR spectroscopy, 2 ed. Heilbronn: SPS Verlagsgesellschaft, 2007.
11. Moolenaar SH, van der Knaap MS, Engelke UF, Pouwels PJ, Janssen Zijlstra FS, Verhoeven NM, Jakobs C, Wevers RA. In vivo and in vitro NMR spectroscopy reveal a putative novel inborn error involving polyol metabolism. *NMR Biomed* 2001;14:167-76.
12. Valayannopoulos V, Verhoeven NM, Mention K, Salomons GS, Sommelet D, Gonzales M, Touati G, de Lonlay P., Jakobs C, Saudubray JM. Transaldolase deficiency: a new cause of hydrops fetalis and neonatal multi-organ disease. *J Pediatr* 2006;149:713-7.
13. La Forge FB, Hudson CS. Sedoheptose, a new sugar from *Sedum spectabile*. *Journal of Biological Chemistry* 1917;30:61-77.

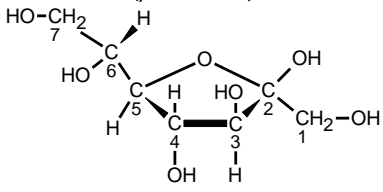
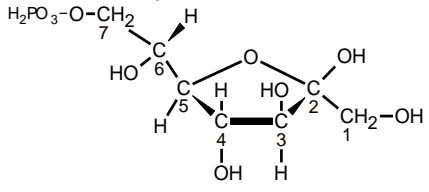
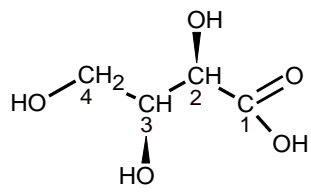
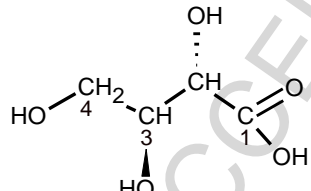
14. Engelke UF, Kremer B, Kluijtmans LA, van der Graaf M, Morava E, Loupatty FJ, Wanders RJ, Moskau D, Loss S, van den Bergh E, Wevers RA. NMR spectroscopic studies on the late onset form of 3-methylglutaconic aciduria type I and other defects in leucine metabolism. *NMR Biomed* 2006;19:271-8.
15. Charmantray F, Helaine V, Legeret B, Hecquet L. Preparative scale enzymatic synthesis of D-sedoheptulose-7-phosphate from beta-hydroxypyruvate and D-ribose-5-phosphate. *Journal of Molecular Catalysis B: Enzymatic* 2008;57:6-9.
16. Kuchel PW, Berthon HA, Bubb WA, McIntyre LM, Nygh NK, Thorburn DR. <sup>13</sup>C and <sup>31</sup>P NMR studies of the pentose phosphate pathway in human erythrocytes. *Biomed Biochim Acta* 1990;49:S105-S110.
17. A.C.Soria, M.L.Sanz, M.Villamiel. Determination of minor carbohydrates in carrot (*Daucus carota* L.) by GC-MS. *Analytical Methods* 2009;114:758-62.
18. Takuo Okuda, Setsuo Saito, Masayuki Hayashi. Trimethylsilylation and G.L.C.-mass spectrometry of 3-ketoses and 2-heptuloses. *Carbohydrate Research* 1997;68:1-13.
19. Guneral F, Bachmann C. Age-related reference values for urinary organic acids in a healthy Turkish pediatric population. *Clin Chem* 1994;40:862-6.
20. Blau N, Duran M, Blaskovics ME, Gibson KM. *Physician's guide to the laboratory diagnostics of metabolic diseases*, 2 ed. Berlin Heidelberg: Springer-Verlag, 2003.
21. Moolenaar SH, Engelke UF, Wevers RA. Proton nuclear magnetic resonance spectroscopy of body fluids in the field of inborn errors of metabolism. *Ann Clin Biochem* 2003;40:16-24.
22. Kardon T, Stroobant V, Veiga-da-Cunha M, Schaftingen EV. Characterization of mammalian sedoheptulokinase and mechanism of formation of erythritol in sedoheptulokinase deficiency. *FEBS Lett* 2008;582:3330-4.
23. Hauschildt S, Chalmers RA, Lawson AM, Schultis K, Watts RW. Metabolic investigations after xylitol infusion in human subjects. *Am J Clin Nutr* 1976;29:258-73.
24. Ryzlak MT, Pietruszko R. Heterogeneity of glyceraldehyde-3-phosphate dehydrogenase from human brain. *Biochim Biophys Acta* 1988;954:309-24.
25. Ishii Y, Hashimoto T, Minakami S, Yoshikawa H. The formation of erythronic acid 4-phosphate from erythrose 4-phosphate by glyceraldehyde-3-phosphate dehydrogenase. *J Biochem* 1964;56:111-2.
26. Wehrli SL, Berry GT, Palmieri M, Mazur A, Elsas L, Segal S. Urinary galactonate in patients with galactosemia: quantitation by nuclear magnetic resonance spectroscopy. *Pediatr Res* 1997;42:855-61.
27. Hanczko R, Fernandez DR, Doherty E, Qian Y, Vas G, Niland B, Telarico T, Garba A, Banerjee S, Middleton FA, Barrett D, Barcza M, Banki K, Landas SK, Perl A. Prevention of hepatocarcinogenesis and increased susceptibility to acetaminophen-induced liver failure in transaldolase-deficient mice by N-acetylcysteine. *J Clin Invest* 2009;119:1546-57.

**Table 1** Concentrations ( $\mu\text{mol}/\text{mmol}$  creatinine) of metabolites found in the urine from patients with TALDO deficiency.

Patient	Age <sup>a</sup>	Sedoheptulose <sup>b</sup> ( $\beta$ -furanose)	Erythronic acid <sup>b</sup>	Erythritol <sup>c</sup>	Ribitol <sup>c</sup>	Arabitol <sup>c</sup>	Oxoglutaric acid <sup>b</sup>	Fumaric acid <sup>b</sup>
1	16y	390	550	137	67	142	130	42
2 <sup>d</sup>	1m	1700	2900	1058	234	345	nd	20
3 <sup>d</sup>	4y	160	770	205	41	192	50	44
4 <sup>e</sup>	3y	290	350	217	167	253	280	8
5 <sup>e</sup>	1y	870	670	494	208	298	440	8
6	4y	350	350	290	137	262	1090	110
R	0-3m	<40 [6]	<120	58-162 [9]	7-16 [9]	27-97 [9]		
R	1-2y	<10 [6]	<50	76-192 [9]	9-24 [9]	52-88 [9]		
R	2-6y	<10 [6]	<50	55-104 [9]	8-11 [9]	32-78 [9]		
R	18-80y	<10 [6]	<50	19-76 [9]	2-5 [9]	10-44 [9]		
R	$\leq$ 5y						30-117 [20]	4-10 [20]
R	>5y						2-95 [20]	nd-4 [20]

<sup>a</sup> y, year(s), m, month(s); <sup>b</sup> Analyzed by <sup>1</sup>H-NMR; <sup>c</sup> Analyzed by GC-MS; <sup>d,e</sup> Sibs from 2 different families; R, Reference range; nd, not detectable

**Table 2** <sup>1</sup>H-NMR assignments for sedoheptulose, sedoheptulose 7-phosphate, threonic acid and erythronic acid.

Metabolite	Pos	Multiplicity*	Chemical shift (ppm)	
			pH 2.50	pH 7.00
Sedoheptulose ( $\beta$ -furanose) 	1	AB	3.55	3.58
	3	D	4.08	4.09
	4	DD	4.29	4.31
	5	M	3.75	3.77
	6,7	several	3.85-3.80	3.8
Sedoheptulose 7-phosphate ( $\beta$ -furanose) 	1	AB	3.56	3.54 [15]
	3	D	4.08	4.06 [15]
	4	DD	4.32	4.33 [15]
	5	M	3.81	3.78 [15]
	6,7	several	3.92	3.93 [15]
Threonic acid 	2	D	4.33	4.10
	3	M	4.07	3.98
	4	M	3.68	3.66
Erythronic acid 	2	D	4.32	4.10
	3	M	3.99	3.96
	4	M	3.69	3.66

Pos, carbon position in the molecule

\*, D, doublet; M, multiplet; AB, AB system; DD, doublet-doublet

Figure legends

**Figure 1 Sedoheptulose purified from *Sedum spectabile* “Brillant”.**

**A.** 500 MHz  $^1\text{H}$ -NMR spectrum. Assignments “S” refer to the most prominent anomeric form of sedoheptulose,  $\beta$ -furanose. Subscript numbers refer to the carbon position in the molecule. Assignments ★ refer the other anomeric forms of sedoheptulose.

**B.** GC profile: Pooled urine spiked with purified sedoheptulose. Sedoheptulose anomers were present in a ratio furanose-1: furanose-2: pyranose-1: pyranose-2 = 22%:64%:8%:6%. In all likelihood furanose-1 and pyranose-1 are alfa-forms and furanose-2 and pyranose-2 are the beta forms.

**C1.** Mass spectrum for the peak with assignment furanose-2 (m/z values {relative abundance}: 73{100}, 217{45}, 147{27}, 204{18} and 359{15}). Characteristic for the furanose forms is the low ratio for m/z 204 : m/z 217 [18].

**C2.** Mass spectrum for the peak with assignment pyranose-2 (m/z values {relative abundance}: 73{100}, 204{62}, 147{26}, 359{22} and 217{12}). Characteristic for the pyranose forms is the high ratio for m/z 204 : m/z 217 [18].

**Figure 2. *In vitro*  $^1\text{H}$ -NMR spectra (500 MHz) of urine and model compounds measured at pH 2.50.**

- A. Threonic acid
- B. Erythronic acid
- C. Sedoheptulose isolated from *sedum spectabile*
- D. Urine of a patient with transaldolase deficiency (S=sedoheptulose and E=erythronic acid. Subscript numbers refer to the carbon position in the molecule [Table 2])

**Figure 3. GC MS chromatogram of urine.**

- A. Pooled urine spiked with erythronic acid.
- B. Urine of patient with transaldolase deficiency
- C. Control urine
- D. Mass spectrum of erythronic acid in the urine of the TALDO patient

**Figure 4. *In vitro*  $^1\text{H}$ -NMR spectra (500 MHz) of urine from mice measured at pH 2.50.**

- A. Urine of a control mouse
- B. Urine of a mouse with transaldolase deficiency (S=sedoheptulose and E=erythronic acid. Subscript numbers refer to the carbon position in the molecule [Table 2])

**Figure 5. Pentose Phosphate Pathway**

Transaldolase deficiency (Solid black square) results in accumulation of sedoheptulose, erythritol and erythronic acid.

- 1, Transaldolase
- 2, Sedoheptulokinase
- 3, Cytosolic phosphatase
- 4, Fructokinase
- 5, Aldolase B
- 6, Aldehyde reductase
- 7, Putative (after Hauschildt et al [23])

8, Glyceraldehyde 3-phosphate dehydrogenase [24;25]

9, Phosphatase

10, Putative [26]

11, Transketolase

12, D-Ribulose 5-phosphate epimerase

13, Ribose 5-phosphate isomerase

ACCEPTED MANUSCRIPT

Figure 1

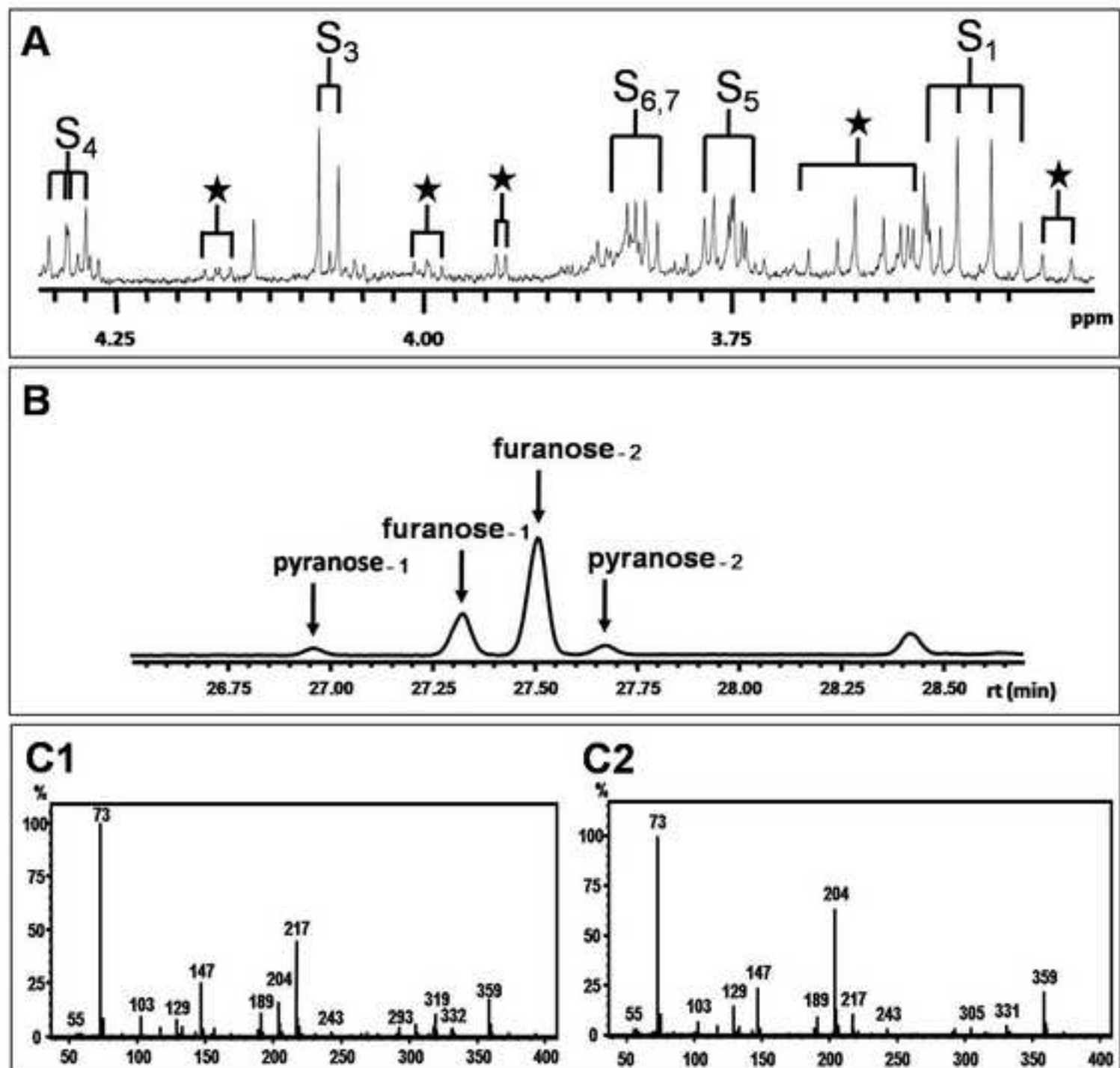
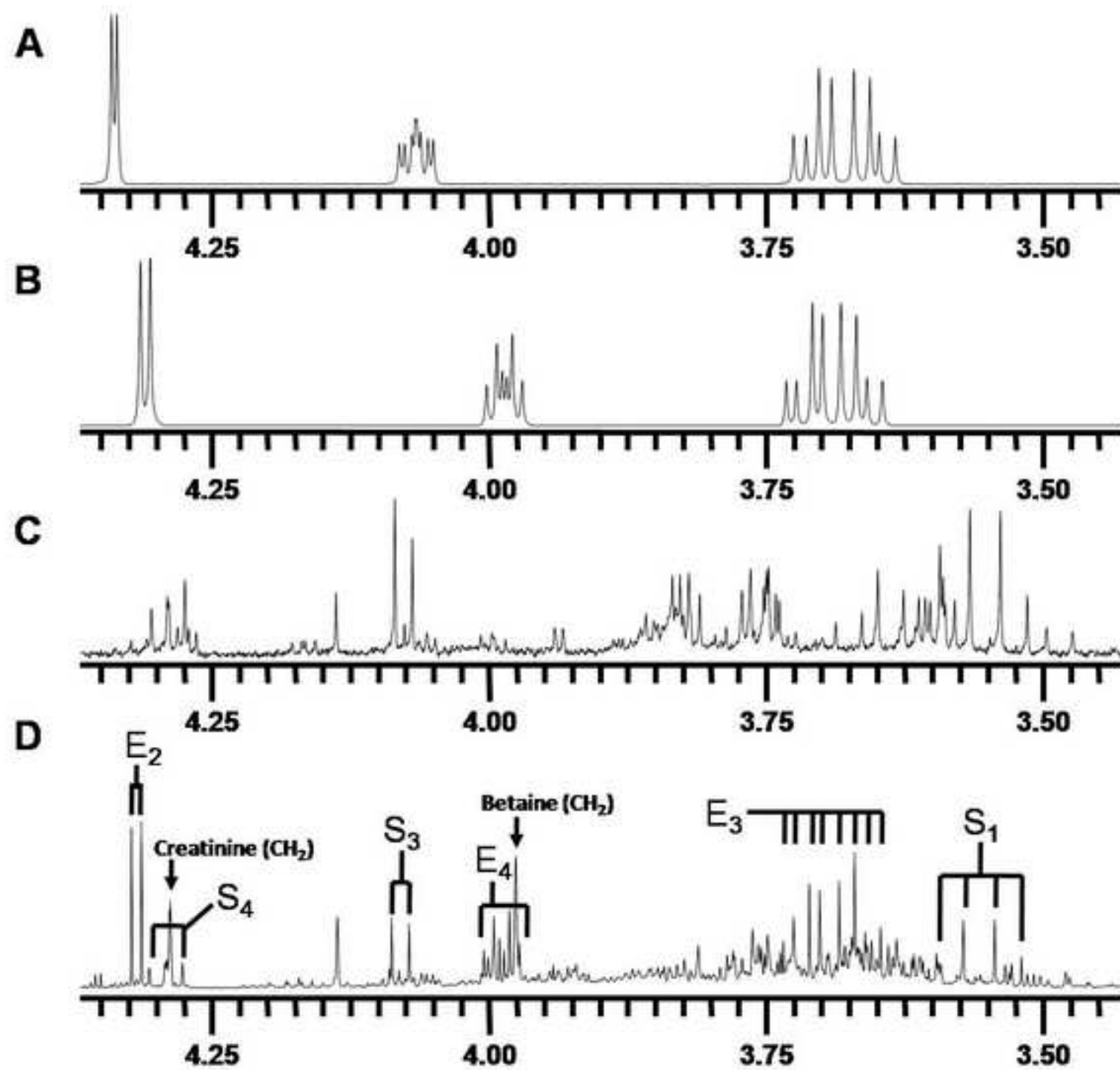
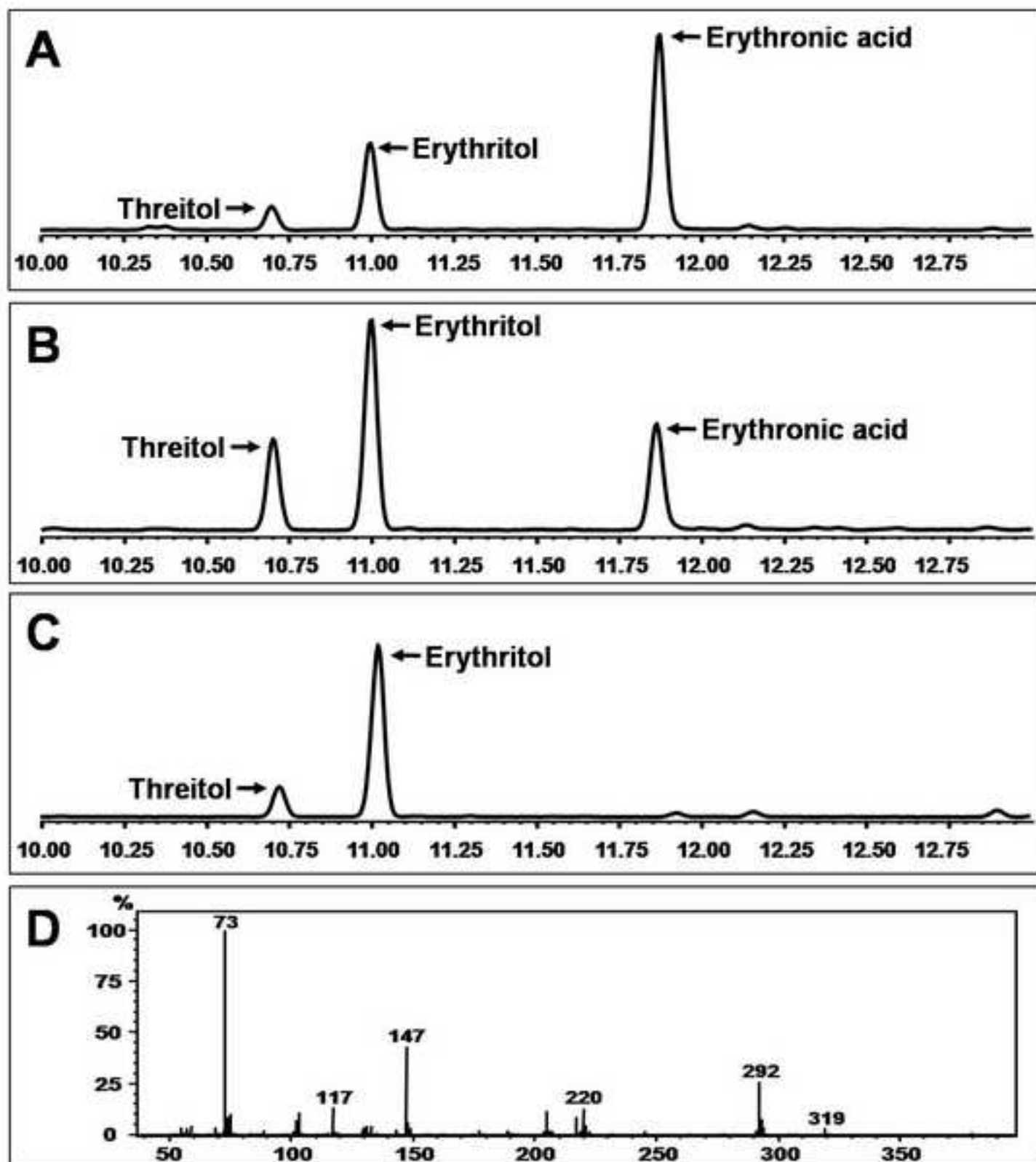


Figure 2





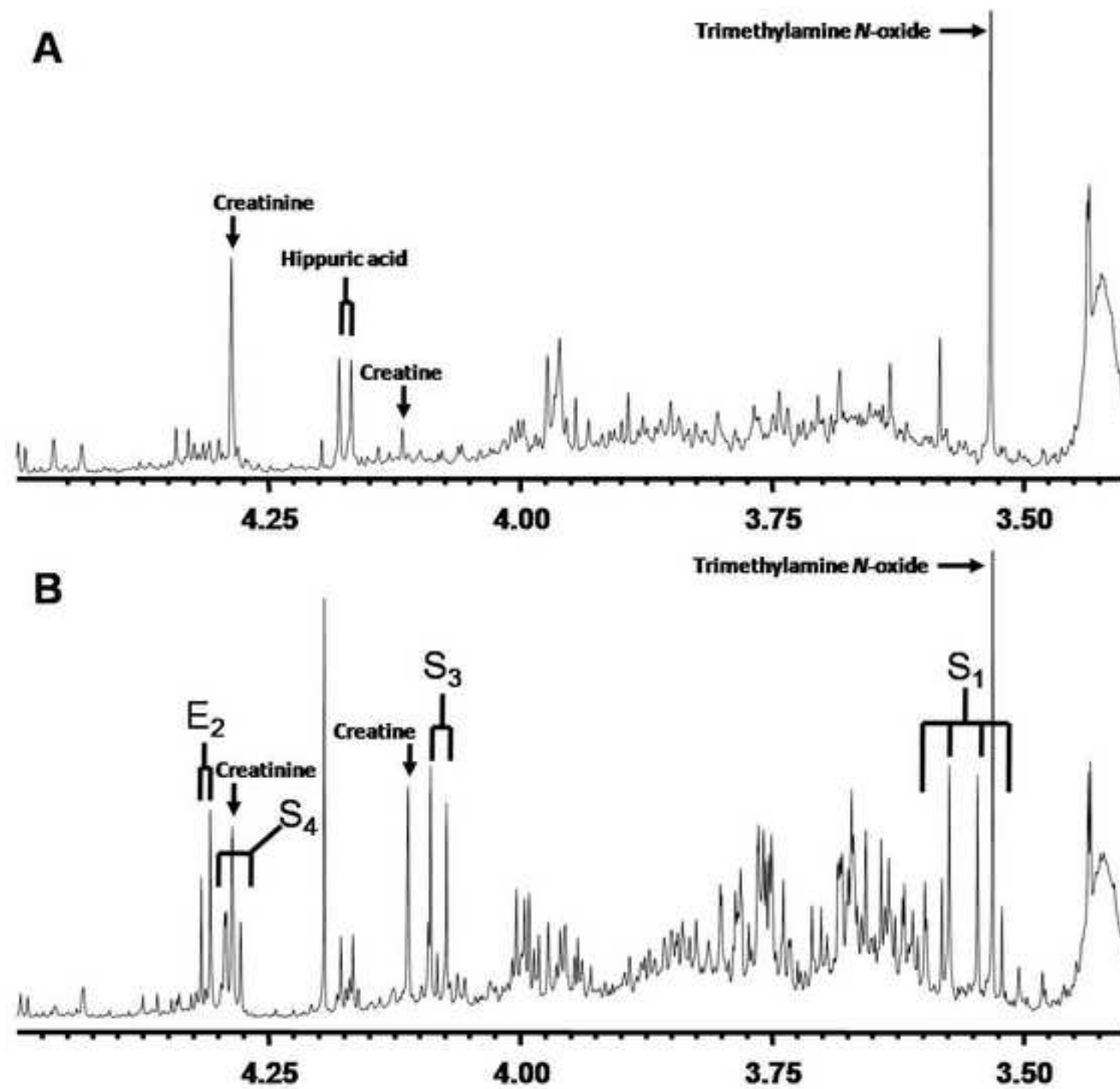


Figure 5

